Original article

Inhibition of anti-inflammatory pathway through suppressors of cytokine signalling (Socs2/Socs3) in the initiation of hepatocellular carcinoma

Isbah Ashfaq [a,b], Nadeem Sheikh [a], Naz Fatima [a,c], Asima Tayyeb [b,*]

[a] Cell & Molecular Biology Lab, Institute of Zoology, University of the Punjab, Quaid-i-Azam Campus, Lahore 54590, Pakistan
[b] School of Biological Sciences (SBS), University of the Punjab, Quaid-i-Azam Campus, Lahore 54590, Pakistan
[c] Department of Zoology, Faculty of Science and Technology, University of Central Punjab, Lahore, Pakistan

ARTICLE INFO

ABSTRACT

Hepatocellular carcinoma (HCC), a leading cause of cancer related deaths is predominantly driven by chronic inflammatory responses. Due to asymptomatic nature and lack of early patient biopsies, precise involvement of inflammation in hepatic injury initiation remains unidentified. Aim of the study was to elucidate the regulation patterns of inflammatory signalling from initiation of hepatic injury to development of HCC. HCC mice model was established using DEN followed by repeated doses of CCl_4 and sacrificed at three different stages of disease comprising 7, 14 and 21 weeks. Serum biochemical tests, hepatic lipids quantification, histopathology and qPCR analyses were conducted to characterize the initiation and progression of liver injury and inflammatory signalling. Notably, at 7 weeks, we observed hepatocyte damage and periportal necrotic bodies coupled with induction of Socs2/Socs3 and anti-inflammatory cytokine Il-10. At 14 weeks, mice liver showed advancement of liver injury with micro-vesicular steatosis and moderate collagen deposition around portal zone. With progression of injury, the expression of Socs3 was declined with further reduction of Il-10 and Tgf-β indicating the disturbance of anti-inflammatory mechanism. In contrast, pro-inflammatory cytokines Il1-β, Il6 and Tnf-α were upregulated contributing inflammation. Subsequently, at 21 weeks severe liver damage was estimated as characterized by macro-vesicular steatosis, perisinusoidal collagen bridging, immune cell recruitment and significant upregulation of Col-1α and α-Sma. In parallel, there was significant upregulation of pro/anti-inflammatory cytokines highlighting the commencement of chronic inflammation.

Findings of the study suggest that differential regulation of cytokine suppressors and inflammatory cytokines might play role in the initiation and progression of hepatic injury leading towards HCC.

© 2022 Published by Elsevier B.V. on behalf of King Saud University. This is an open access article under the CC BY-NC-ND license (http://creativecommons.org/licenses/by-nc-nd/4.0/).

1. Introduction

Hepatocellular carcinoma (HCC) is the fourth most common cause of cancer related mortality worldwide. The prevalence of HCC is increasing significantly with an estimated 905,677 new cases reported in 2020 (Kim and Viatour 2020, Sung et al., 2021).

Production and hosting by Elsevier

HCC pathogenesis is a complex and multi-step process driven by the progressive accumulation of cellular and molecular etiologies (Jafri and Kamran, 2019, Suresh et al., 2020). Adipokine secretion, endoplasmic reticulum stress, oxidative stress, mitochondrial dysfunction, inflammation and hepatocytes necrosis or apoptosis emerged as key driving factors of HCC. Despite significant involvement in HCC, their role at early stages of liver injury are poorly characterized (Irshad et al., 2017, Ghemrawi et al., 2018, Yang et al., 2019).

Inflammation is a natural phenomenon mainly triggered by diverse factors including cellular damage, toxins and pathogens (Chen et al., 2018). These factors may elicit inflammatory responses characterized by recruitment of inflammatory cells and induction of inflammatory signalling pathways at the site of injury. Normally, these responses work together to repair tissue, resist harmful stimuli and resolve homeostasis. However, under some

Abbreviation

Hepatocellular carcinoma	HCC	Krt-18	Cytokeratin-18
Di-ethyl-nitrosamine	DEN	Alb	Albumin
Carbon tetrachloride	CCl_4	β-actin	Beta actin
Cytochrome P450	CYP	Col-1α	Collagen-1α
Weeks	W	Il1-β	Interleukin-1β
Vehicle control	VC	Il6	Interleukin 6
Intraperitoneally	IP	Myd88	Myeloid differentiation primary response
Alanine aminotransferase	ALT	Tlr	Toll-Like receptors
Aspartate aminotransferase	AST	Tgf-β	Transforming Growth Factor- β
Triglycerides	TGs	Tnf-α	Tumour Necrosis Factor- α
H&E	Hematoxylin & Eosin	NAFLD	Non-alcholic fatty liver disease
MT	Masson's Trichrome		
Quantitative polymerase chain reaction	qPCR		

circumstances, obstinate inflammatory response results in the aberrant production of pro and anti-inflammatory cytokines and dysregulation of inflammatory modulators leading to chronic inflammation (Yu et al., 2018). Chronic inflammation initiates a crosstalk among different types of liver cell and its microenvironment resulting in complete remodelling of liver architecture (Refolo et al., 2020). Thus, understanding the relationship between inflammatory mediators and inflammatory responses may present as a potent target for HCC prevention and therapy.

Suppressors of cytokine signalling (SOCS) is an intracellular protein family which functions as basic physiological regulator of cytokine signalling. The key biological function of SOCS is to mediate cytokine signalling through negative feedback mechanism (Ye and Driver 2016). Dysregulation of SOCS has also emerged as essential modulator of inflammatory and oncogenic proliferation pathways. Depending on the biological and cellular conditions, SOCS may serve as an oncogene or a tumour suppressor (Jiang et al., 2017, Sobah et al., 2021). Studies have further showed SOCS3, an important member of the family increases phosphorylation of the oncogenic pathways such as IL-6/JAK/STAT3 in human HCC (Lokau et al., 2019). Owing to its double edged role of SOCS, its comprehensive analysis is required to control inflammatory signalling involved in the development of HCC.

A variety of genetically modified, xenograft-based, transgenic, and hepatotoxicant-induced mice models are being used to study the pathogenesis of HCC (Zhang et al., 2019a). Recently, two-stage animal models were employed in which a genotoxicant such as di-ethyl-nitrosamine (DEN) was first administered to induce tumour followed by a tumour promoting hepatotoxicant (Omura et al., 2014). These models are well appropriate for studying the molecular mechanisms behind the activation of pro-inflammatory mediators and the suppression of anti-inflammatory signalling cascades (Stanke-Labesque et al., 2020).

The current study was aimed to elucidate the regulation of inflammatory signalling in the initiation and progression of hepatic injury. Liver injury to HCC mouse model was established using DEN and CCl_4. Results of the study has highlighted the critical role of expressional fine-tuning of inflammatory signalling and its modulators in the pathogenesis of HCC.

2. Material and methods

2.1. Animals

Laboratory Mice BALB/c were used for experiment. Mice were nurtured in animal house according to ethical guidelines for animal care in SBS, University of the Punjab, Quaid-i-Azam campus, Lahore, Pakistan. Mice were kept in clean cages with saw under 12/12 h light/dark cycles at 25 ± 2°C ambient temperature and were fed commercially available standard chow and water ad libitum.

2.2. Establishment of HCC mice model

The healthy male mice (6 weeks old) weighing up to 25 ± 5 g were randomly grouped into six (8 males/group n = 8) for establishment of DEN + CCl_4 induced HCC model. Each group of mice was either administered DEN + CCl_4 or saline/olive oil for 7, 14 and 21 weeks (W). For chemical induction of HCC, mice in experimental groups were treated with first dose of DEN (100 mg/kg) with repeated dose of carbon tetrachloride (CCl_4) (0.5 ml/kg) twice a week for 2 weeks. After 2 weeks second dose of DEN (50 mg/kg) was administered to mice and repeated dose of CCl_4 (0.5 ml/kg) twice a week was continued for 7, 14 and 21 weeks (Injury; 7 W, 14 W and 21 W). Solution of DEN was made in saline whereas CCl_4 was dissolved in olive oil (1:1, v/v). All doses were administered intraperitoneally (IP). In parallel to all vehicle control groups (VC; 7 W, 14 W and 21 W) saline and olive oil were administered (IP) per body weight as alternative of DEN and CCl_4. During experimental period, body weight of all the mice were measured twice a week. Schematic experimental timeline is represented in Fig. 1.

2.3. Sample collection and processing

By the end of 7, 14 and 21 weeks experiments, under proper anaesthesia (ketamine/xylazine cocktail, IP), mice were scarified followed by blood collection in nonheparinized tubes and serum separation using centrifuge machine (4000 × g, 20 min). The straw coloured serum was stored and used to measure liver function test. Liver organ was separated, washed with phosphate buffer saline and chopped for histological analyses, lipid assay and gene expression analyses.

2.4. Liver biochemical test

The activity of alanine aminotransferase (ALT) and aspartate aminotransferase (AST) was measured in serum sample from each group. The assays were performed by calorimetric method, using commercially available kits. Briefly, 50 μL of serum samples were preincubated in 1 ml of working reagents for 1 min at 37 °C and added in a cuvette. Initial absorbance was measured at 340 nm in spectrophotometer and absorbance readings were repeatedly measured exactly after 1, 2 and 3 min. Relative average change in absorbance per minute was calculated.
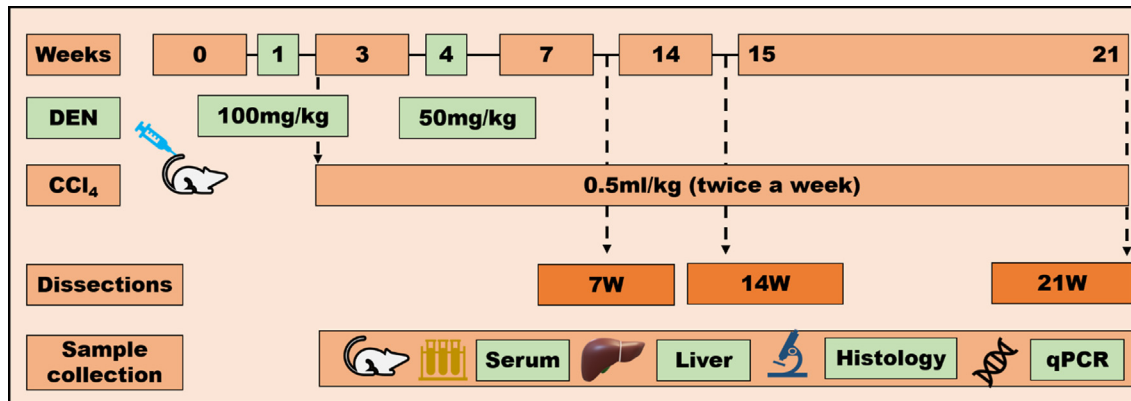
Fig. 1. A representation of experimental timeline.

2.5. Hepatic lipid extraction

Hepatic lipid content was extracted according to modified Bligh and Dyer method (Bligh and Dyer 1959) as described previously (Perveen et al., 2020). Briefly, 12 mg of liver was used for extraction of cholesterol and triglycerides (TGs). Liver homogenate was made in $MgCl_2$ (1 M) and chloroform–methanol (2:1) in a micro-tube. The chloroform phase was recovered, vacuum dried and quantified using commercially available kit (Analyticon biotechnologies). Both cholesterol and TGs in each sample were separately determined.

2.6. Assessment of liver gross morphology

The body weight of mice was recorded in respective groups. Liver was separated, weighed and then examined for the presence of grossly visible lesions.

2.7. Histopathological examination of liver architecture

The one-half of mice liver tissue was fixed in 4% paraformaldehyde (PFA) solution overnight. Tissues were subjected to dehydration using ascending grades of ethanol and embedded in paraffin

Table 1
Mice's primer sequences, annealing temperature (Tm) and size.

Gene I.D	Primer	Primer sequences (5′-3′)	Tm (C)	Size (bp)
β-actin	Forward	GAAGTCCCTCACCCTCCCAA	57	62
	Reverse	GGCATGGACGCGACCAT		
Alb	Forward	GAAGTGCTCCAGTATGCAGAA	57	222
	Reverse	GAGATAGTCGCCTGGTTTTCAC		
Krt18	Forward	GAAGAGCCTGGAAACTGAGAAC	57	150
	Reverse	TTGTCCACAGAATTCGCAAAGA		
Col-1α	Forward	TGAGTCAGCAGATTGAGAAC	57	301
	Reverse	TACTTCGAACGGGAATCCATC		
α-Sma	Forward	GCATCCACGAAACCACCTA	57	418
	Reverse	CACGAGTAACAAATCAAAGC		
Cyp1a1	Forward	GGTCACTCTCTTTGGTTTGG	54	217
	Reverse	AAGAATGCTGAGGGACCACCAGAAG		
Cyp1a2	Forward	CGTTCTCCCAGTACATCTCC	54	187
	Reverse	AGTGACAGGTGTGGGTTCTT		
Cyp2e1	Forward	GGAATGGGGAAACAGGGTAATG	57	147
	Reverse	CATGAGCTCCAGACACTTCTTG		
Socs2	Forward	TCAGCTGGACCGACTAACCT	57	150
	Reverse	TGTCCGTTTATCCTTGCACA		
Socs3	Forward	AGCTCCAAAAGCGAGTACCA	57	178
	Reverse	TGACGCTCAACGTGAAGAAG		
Il1-β	Forward	GTACATCAGCACCTCACAAG	57	268
	Reverse	CACAGGCTCTCTTTGAACAG		
Il6	Forward	CCAGAAACCGCTATGAAGTTCC	57	73
	Reverse	TCACCAGCATCAGTCCCAAG		
Il-10	Forward	TGTGAAAATAAGAGCAAGGCAGTG	59	85
	Reverse	CATTCATGGCCTTGTAGACACC		
Tlr4	Forward	TCCCTGCATAGAGGTAGTTC	57	268
	Reverse	ACTCTGGATAGGGTTTCCTG		
Tlr9	Forward	GCCTCCGAGACAACTACCTA	57	210
	Reverse	CTGCTGACATCCAGTTTCTG		
Myd88	Forward	GGCATCTGCATATGTGTGTT	57	223
	Reverse	CCCAGGCTGACCTTAAACTA		
Tnf-α	Forward	CTCCAGGCGGTGCCTATGT	57	67
	Reverse	GAAGAGCGTGGTGGCCC		
Tgf-β	Forward	CCCGAAGCGGACTACTATGC	57	69
	Reverse	ATAGATGGCGTTGTTGCGGT		

wax. Afterwards microtome was used to cut samples into 4 μm thick sections. Liver pathological state was assessed by H&E and Masson's trichrome (MT) staining. NAFLD activity score (NAS) method was used to evaluate different stages of liver pathogenesis. The Olympus IX83 inverted fluorescent microscope was used to snap microphotographs of four stained biological replicates.

2.8. RNA isolation and cDNA synthesis

To carry out gene expression analysis the total mRNA was isolated from liver tissues using RiboEX™ kit (Gene all, catalogue no. 305–101) following manufacturer's protocol. RNA quantity and quality were determined at 260/280 ratio using nanodrop spectrophotometer (Thermo Scientific). The cDNA for each sample was synthesized from 2 μg RNA using revert aid first strand cDNA synthesis kit (Thermo Scientific, catalogue no. K1622) by following manufacturer's instructions. All cDNA samples were stored at -20^0C.

2.9. Gene expression analysis by quantitative polymerase chain reaction (qPCR)

The cDNA was used for quantitative polymerase chain reaction (qPCR) analysis of mRNA by using primers given in Table 1 (Azam et al., 2018). qPCR was then performed with 25 ng cDNA using Maxima SYBR Green kit (Thermo Scientific, catalogue no. k0251) in thermal cycler. Maxima SYBR Green (Thermo Scientific, catalogue no. k0251) was used for master mix preparation. The PikoR-

eal™ Real-Time PCR System (Thermo Scientific, catalogue no. TCR0096) was used, PCR cycling conditions were as follow: initial denaturation at 95 °C and 40 cycles of 95 °C, ±57 °C, and 72 °C followed by final elongation at 72 °C and termination at 4 °C. The Beta-actin (β-actin) as housekeeping gene was analyzed in each sample for normalization and fold changes were determined using $2^{-\Delta\Delta Ct}$ method.

2.10. Data analysis

Data was analysed using one-way analysis of variance (ANOVA) followed by multiple comparison Tukey's post hoc test from Graph Pad Prism 8 and 9. The significance level was considered as $p < 0.05$, $p < 0.01$, $p < 0.001$ and $p < 0.0001$. Results were expressed as mean ± standard error of mean (SEM) and standard deviation (SD).

3. Results

3.1. Stage dependent variations in physiological parameters

The progression of liver injury was assessed by variations in physiological parameters such as weight of body and liver, and gross morphology. Body weight of mice in vehicle control groups (VC) was progressively increased throughout the experimental period. In contrast, a significant reduction in body weight of mice in all treatment groups (Injury; 7 W, 14 W, 21 W) was observed [Fig. 2A]. Results demonstrated that body weight was suddenly
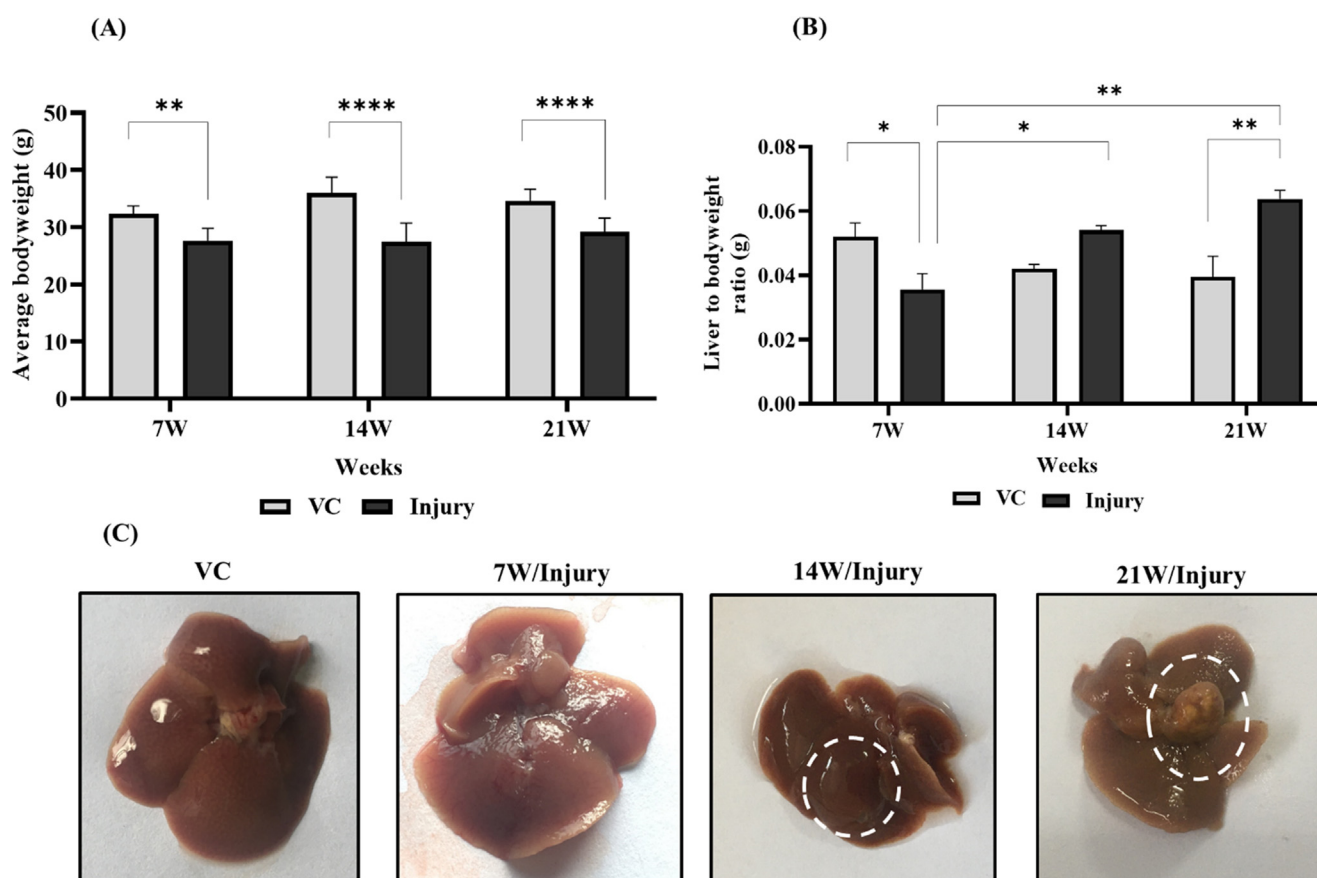
Fig. 2. (A) Shown here decline in bodyweight in injury groups at 7 W, 14 W and 21 W compared to VC groups (B) Increased liver to bodyweight ratio in injury groups at 7 W, 14 W and 21 W relative to vehicle control groups. Significant level was considered as $p < 0.05$, $p < 0.01$, $p < 0.001$ and $p < 0.0001$ and graphical data presented in mean ± S.D.(C) Gross morphology of mice liver showing initiation of tumour formation injury group at 14 W and tumour nodules in injury group at 21 W. Tumours are highlighted with white dotted circles.
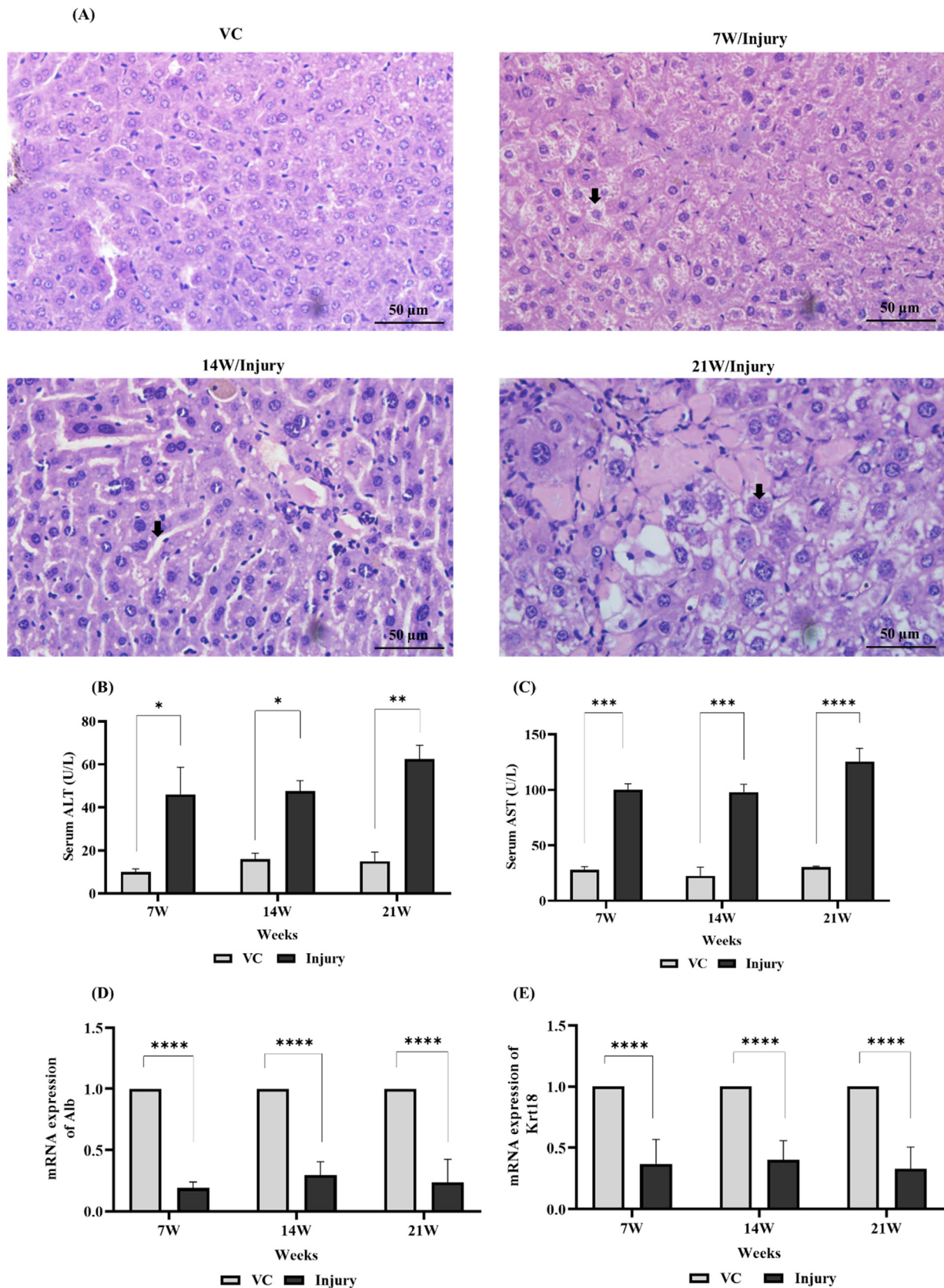
Fig. 3. (A) Represented normal liver architecture of VC group. Black arrowhead in injury groups at 7 W, 14 W and 21 W indicating vacuolation, pyknotic nuclei, necrosis, and sinusoid dilations respectively (20X microphotographs). (B&C) The serum ALT and AST level significantly ($p < 0.05$, $p < 0.01$, $p < 0.001$ and $p < 0.0001$) increased at 7 W, 14 W and 21 W injury groups compared to VC groups. (D&E) mRNA expression of Alb and Krt18 showing significant ($p < 0.0001$) downregulation in injury group at 7 W, 14 W and 21 W compared to VC groups. The graphical data presented in mean ± S.D.

declined in mice of treatment groups after first dose of DEN with a gradual recovery after 10 weeks of treatment and again decreased with last 3 weeks injections of CCl_4 [Supplementary file 1]. Correspondingly, injury groups at 7 W, 14 W and 21 W displayed significant change in liver weight to body weight ratio compared to their VC groups. [Fig. 2B]. Results revealed that relative liver weight to body weight ratio in injury groups at 14 W and 21 W was significantly increased compared to the mice of injury group at 7 W. Moreover, gross morphology of mice liver indicated tumour formation in injury group at 14 W while at 21 W mice liver in injury group exhibited well-differentiated tumour nodules [Fig. 2C]. The survival ratio was 87% until the end of the experiment.

3.2. Initiation of hepatocellular necrosis and impairment of liver function

The onset of hepatocellular injury was characterized by change in liver architecture. Liver sections stained with H&E depicted profound impairments in liver of HCC groups relative to VC groups. Mice exposed to DEN + CCl_4 for 7, 14 and 21 weeks exhibited hepatocyte vacuolation with pyknotic nuclei, necrosis along with sinusoid dilation compared to VC group [Fig. 3A]. Hepatocyte vacuolation and necrosis were more significant in mice of injury group at 21 W. Hepatocellular necrosis was coupled with impairment of liver function as evident by elevation of serum transami-
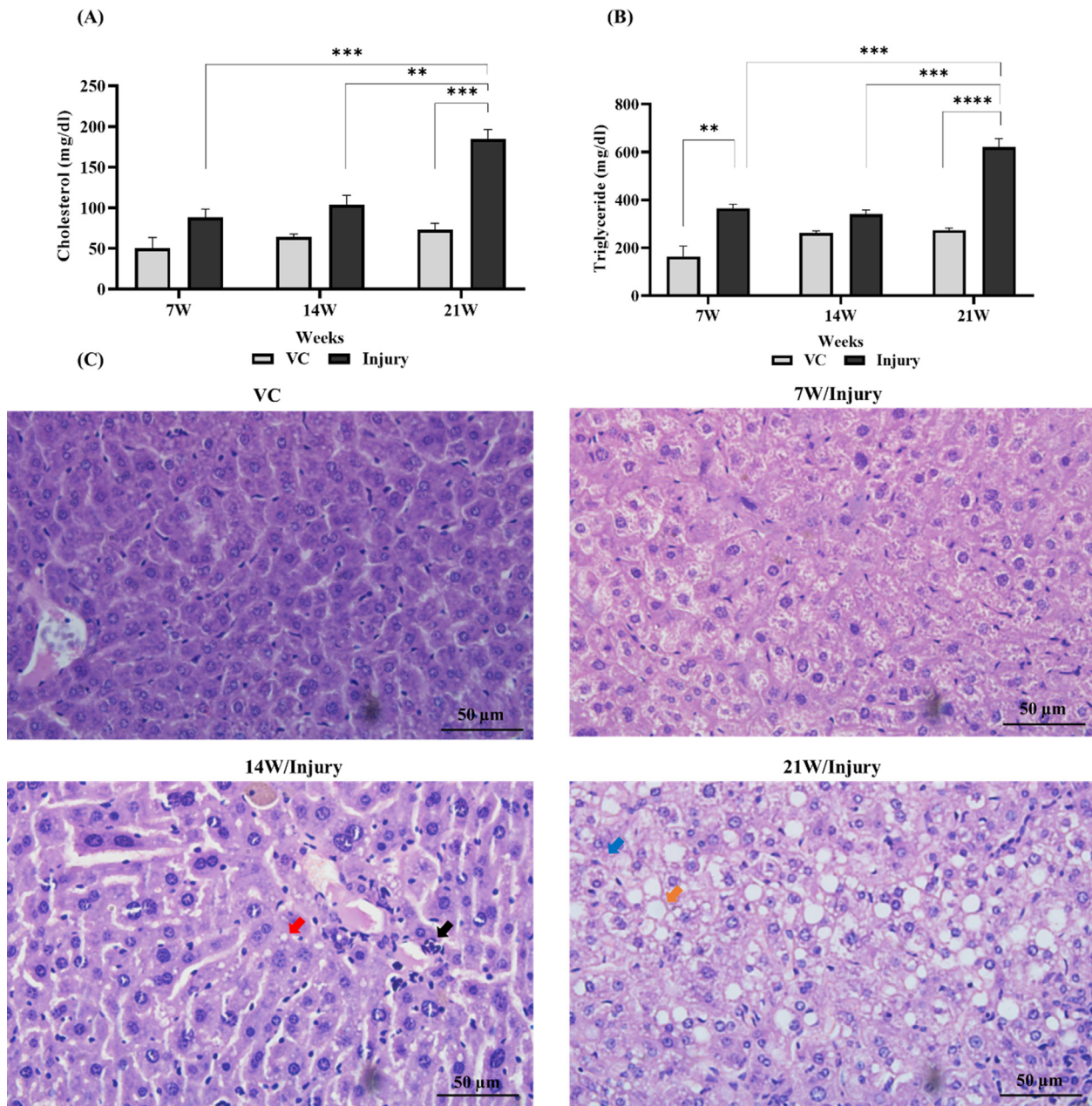

Fig. 4. (A) The graph represented significant increase in cholesterol (mg/dl) in injury group at 21 W (B) Triglycerides concentration was increased significantly at 7 W and 21 W injury groups compared to their respective VC groups. The graphical data presented in mean ± S.D. whereas Significant level was considered as $p < 0.05$, $p < 0.01$, $p < 0.001$ and $p < 0.0001$ (C) Histological architecture of liver showing micro-vesicular steatosis (Red arrow) and lipo-granulomas (Black arrow) in injury group at 14 W. macro-vesicular steatosis (Orange arrow) and Mallory's bodies (Blue arrow) was observed in injury groups at 21 W (20X microphotographs).

nases such as ALT and AST. The results also demonstrated that, mice of injury group at 21 W had higher (35%) levels of ALT compared to mice of injury group at 7 W and 14 W [Fig. 3B]. Similarly, a considerable (25%) elevation of AST was observed in injury group at 21 W compared to injury groups at 7 W and 14 W respectively [Fig. 3C]. These results corroborated by differential regulation of hepatic functional genes like Alb and Krt18. The mRNA expression of Alb and Krt18 was significantly downregulated in injury groups at 7 W, 14 W and 21 groups compared to their VC groups [Fig. 3D, 3E].

3.3. Accumulation of lipids in liver parenchyma followed by induction of severe hepatic steatosis

Hepatic lipid contents such as cholesterol and triglycerides (TGs) were measured to evaluate fatty changes with low dose treatment of DEN + CCl_4 for 7, 14 and 21 weeks. Results demonstrated accumulation of cholesterol and TGs in DEN + CCl_4 treated mice liver. The relative concentration of cholesterol was significantly higher in injury group at 21 W (84.5 mg/dl) than injury groups at 7 W (88.10 mg/dl) and 14 W (103.6 mg/dl) [Fig. 4A]. Sim-
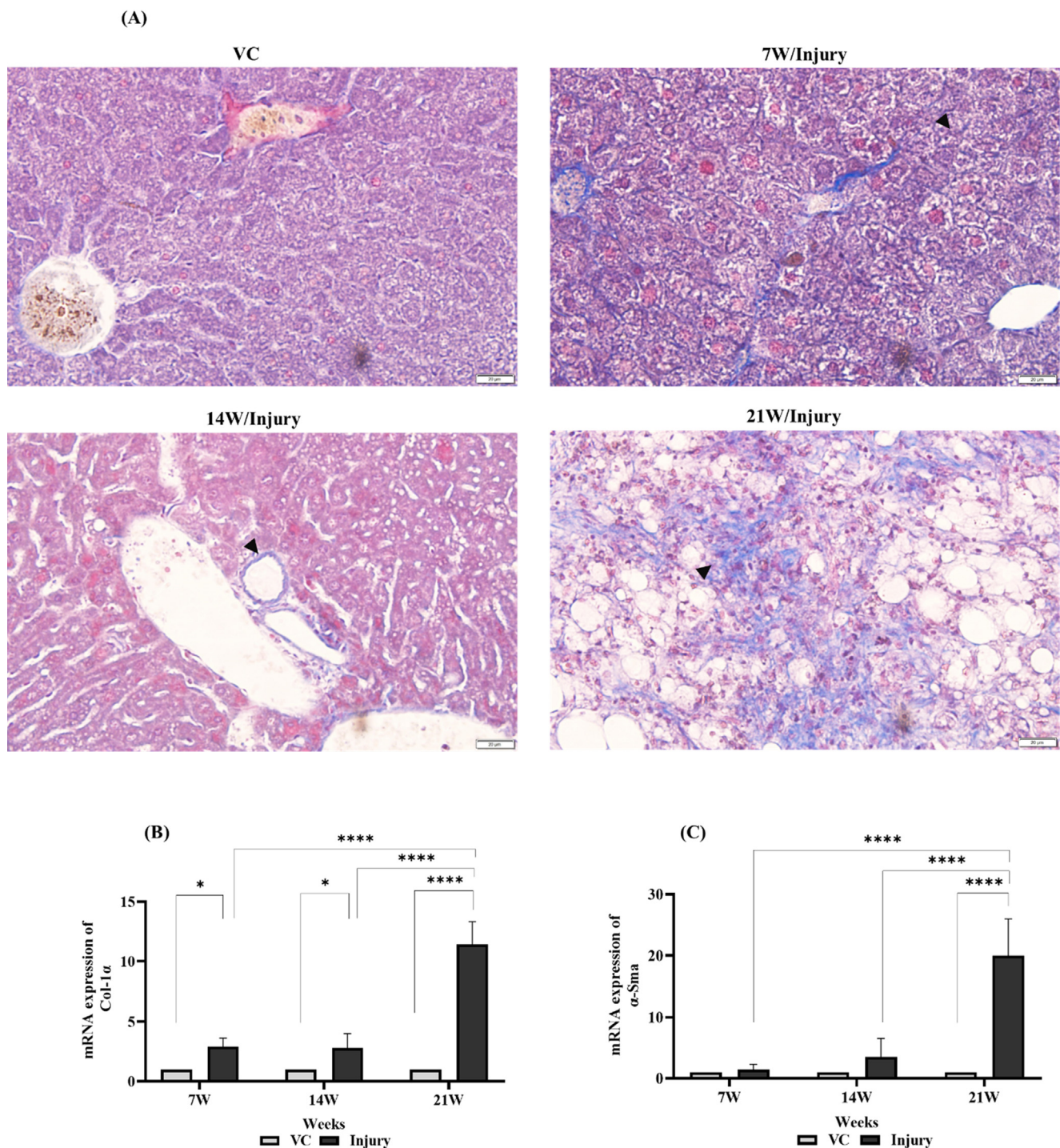
Fig. 5. (A) Collagen deposition in liver sinusoids and periportal fibrosis (Black arrow heads) was observed in injury groups at 7 W, 14 W and 21 W compared to VC group (40X microphotographs). (B) mRNA expression of Col-1α showing continuous increase in collagen expression in injury groups at 7 W, 14 W and 21 W compared to VC groups. (C) Relative expression of mRNA of α-Sma significantly increased at 21 W injury group. The graphical data presented in mean ± S.D.

ilarly, a significant increase in TGs concentration was also observed in injury group at 21 W (621.3 mg/dl) as compared to injury groups at 7 W (365.5 mg/dl) and 14 W (341.1 mg/dl) [Fig. 4B]. In parallel, histopathological analysis of hepatic tissue sections showed gradual progress in hepatocyte degeneration. Results demonstrated that hepatic steatosis initiated with presences of Mallory's bodies and lipo-granulomas after 14 weeks of treatment. The mice of injury group at 14 W showed micro-vesicular steatosis. In contrast, macro-vesicular steatosis was observed in injury group at 21 W [Fig. 4C].

3.4. Fibrogenesis in liver parenchyma progress into HCC

Masson's trichrome staining revealed fibrogenesis in mice exposed to DEN + CCl$_4$ for 7, 14 and 21 weeks. In 7 W (injury group), a network of collagen deposition was exhibited in liver sinusoids and near portal area. Whereas, 14 W (injury group) depicted an accumulation of collagen in steatotic hepatocytes. In 21 W (injury group), periportal, perisinusoidal and bridging fibrosis along with thickness of fibrous bands was more evident [Fig. 5A]. These results were analogue to differential regulation of Col-1α and α-Sma. Where, Col-1α significantly upregulated in injury groups at 7 W, 14 W and 21 W compared to their VC groups [Fig. 5B]. In parallel, regulation of α-Sma was significantly increased in injury group at 21 W compared to VC group at 21 W [Fig. 5C].

3.5. Differential regulation of liver derived cytochrome P450 genes in different stages of liver injury leading to HCC

The mRNA analyses of P450 (Cyp1a1, Cyp1a2 and Cyp2e1) revealed differential expression regulation. In injury group at 21 W, a significant upregulation of Cyp1a1 was observed compared to VC group at 21 W [Fig. 6A]. Whereas, Cyp1a2 and Cyp2e1 significantly downregulated in injury groups at 7 W, 14 W and 21 W compared to their respective VC groups [Fig. 6B, 6C].
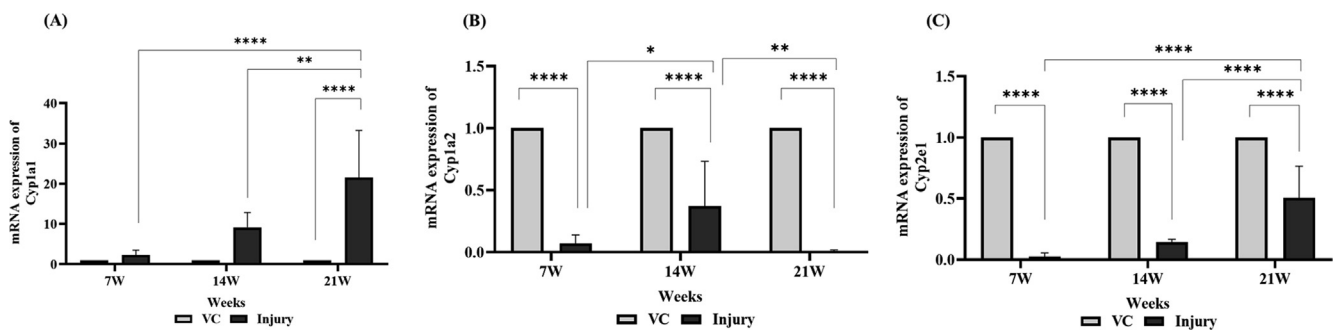
Fig. 6. (A, B&C) The graphical representation of differential expression of Cyp1a1, Cyp1a2 and Cyp2e1 mRNA in injury groups at 7 W, 14 W and 21 W compared to VC groups respectively. The graphical data presented in mean ± S.D. and significant level was considered as $p < 0.05$, $p < 0.01$, $p < 0.001$ and $p < 0.0001$.
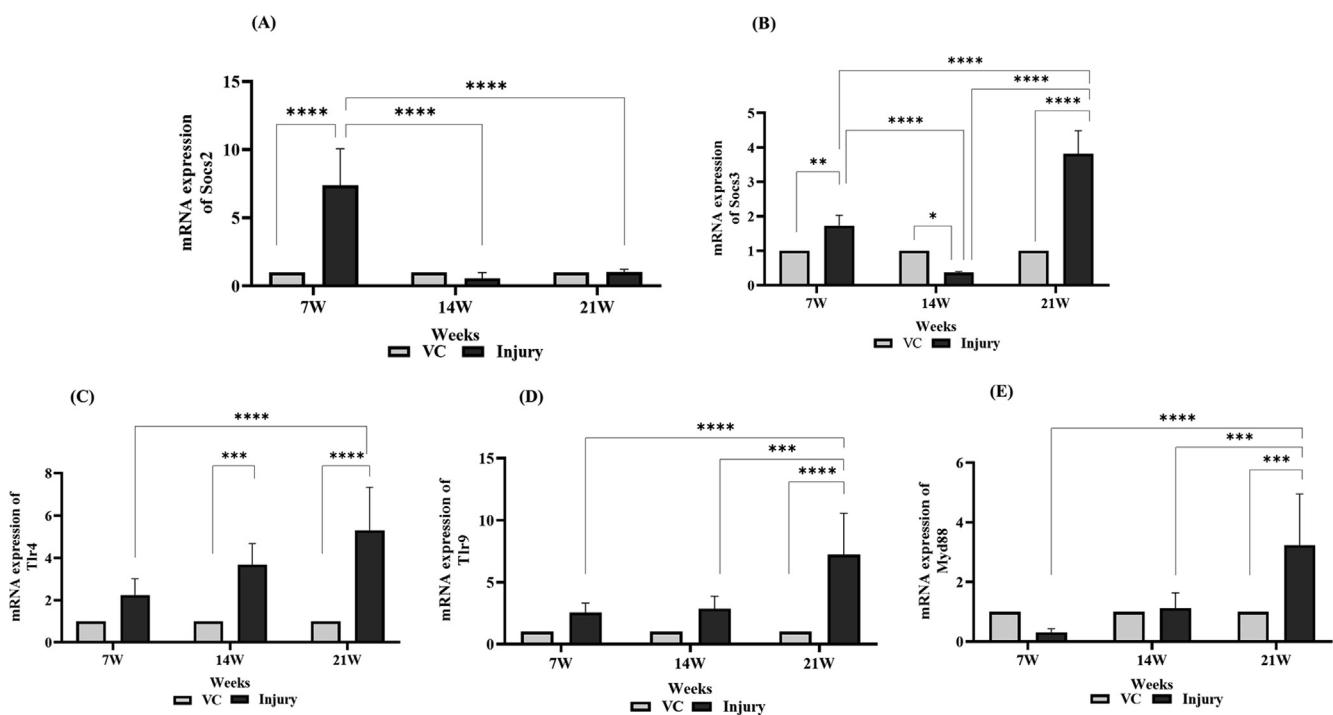
Fig. 7. (A&B) The regulation of suppressor of cytokine signalling (Socs2 and Socs3) was observed at 7 W, 14 W and 21 W in injury groups compared to VC group. (C, D&E) The regulation of Toll-like receptors (Tlr4 and Tlr9) and its adapter molecule (Myd88) was observed in injury groups at 7 W, 14 W and 21 W compared to VC groups respectively. The graphical data presented in mean ± S.D. and significant level was considered as $p < 0.05$, $p < 0.01$, $p < 0.001$ and $p < 0.0001$.

3.6. Differential regulation of suppressor of cytokine signalling (Socs2/Socs3) in different stages of liver injury leading to HCC

The regulation pattern of Socs2 and Socs3 genes showed a variable pattern in different stages of hepatic damage. The mice of injury group at 7 W showed significant upregulation of Socs2 and Socs3 compared to injury groups at 14 W, 21 W and its VC group [Fig. 7A]. Whereas, expression of Socs3 was significantly downregulated in injury group at 14 W group compared to VC group, injury groups at 7 W and 21 W. In contrast, the expression
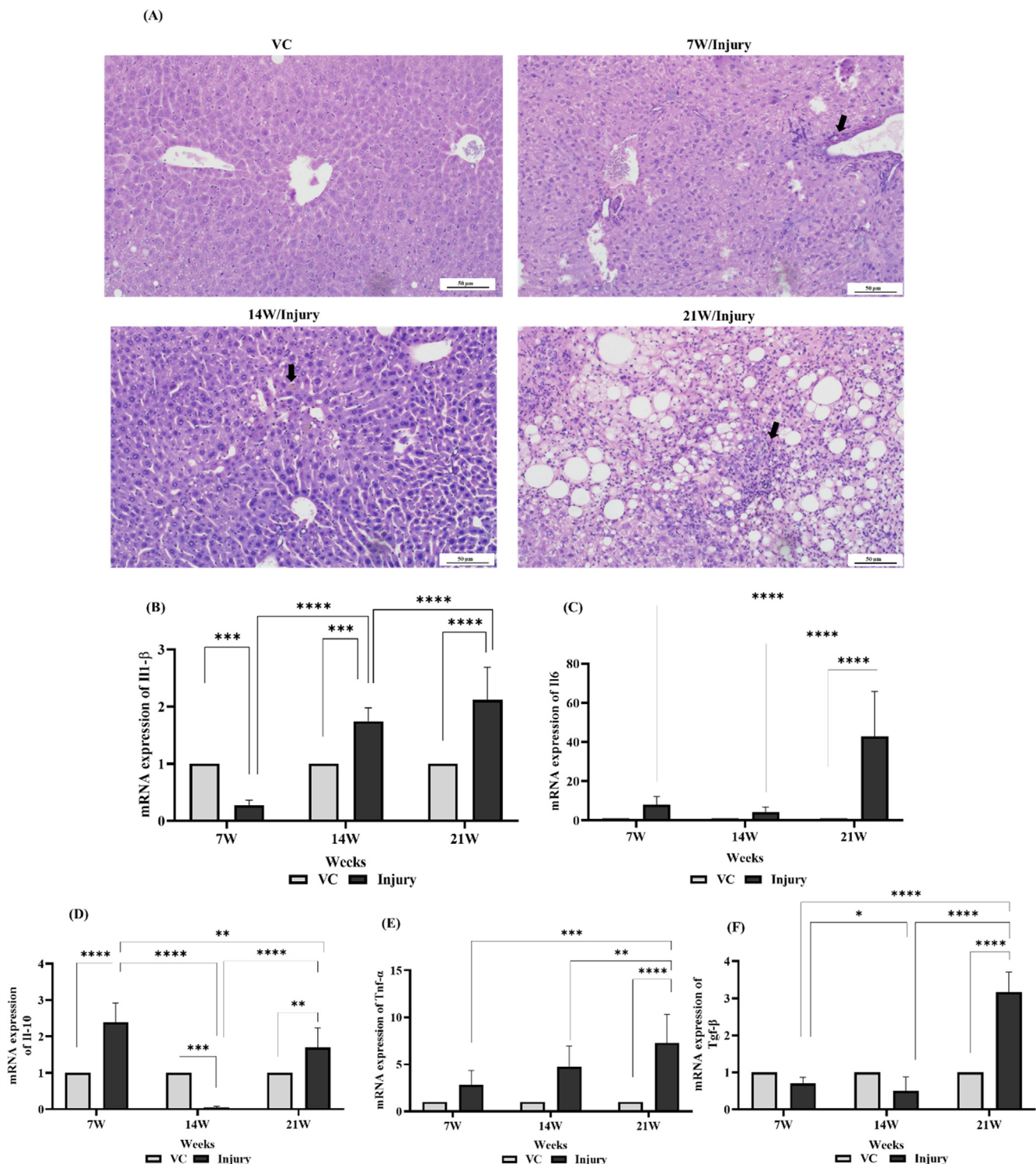
Fig. 8. (A) Histological representation showing lobular inflammation in injury groups at 7 W, 14 W and 21 W compared to VC groups. Periportal necrotic bodies (Black arrow) in injury group at 7 W, pigmented macrophages (Black arrow) in injury group at 14 W and infiltration of inflammatory cells in injury group at 21 W was observed (20X microphotographs). (B, C, D, E&F) Differential expression of Il1-β, Il6, Il-10, Tnf-α and Tgf-β mRNA was observed in injury groups at 7 W, 14 W and 21 W compared to VC groups. The graphical data presented in mean ± S.D. and significant level was considered as $p < 0.05$, $p < 0.01$, $p < 0.001$ and $p < 0.0001$.

of Socs3 was significantly upregulated in advanced stage of hepatic injury group at 21 W compared to both the previous stages as well as its VC [Fig. 7B].

3.7. Differential regulation of Toll-like receptor signalling in late stage of liver injury leading to HCC

The Toll-like receptor signalling genes showed differential regulation patterns in different groups of liver injury. The expression of Tlr4 initiated after 14 weeks. The mice of injury group at 14 W and 21 W showed significant upregulation compared to their VC groups [Fig. 7C]. In contrast, Tlr9 and Myd88 significantly upregulated after 21 weeks compared to their VC groups [Fig. 7E].

3.8. HCC progression followed by induction of inflammatory cytokines

Histopathological examination of the liver sections revealed lobular inflammation, periportal necrotic bodies along with pigmented macrophages and inflammatory cells infiltration in injury groups at 7 W, 14 W and 21 W compared to VC groups [Fig. 8A]. These results were verified by differential regulation of inflammatory cytokines Il1-β, Il6, Il-10, Tnf-α, and Tgf-β. The results demonstrated that expression of Il1-β was significantly downregulated in early stage of hepatic injury (7 W) compared to VC group. A significant upregulation of Il-1β was observed in injury groups at 14 W and 21 W compared to their VC groups [Fig. 8B]. Whereas, Il-10 was significantly upregulated in injury group at 7 W compared to VC group. In contrast, a significant downregulation was observed in mice of injury group at 14 W to VC group. However, Il6, Il-10, Tnf-α and Tgf-β significantly upregulated in injury group at 21 W compared to VC group [Fig. 8C, D, E&F].

4. Discussion

In the current study, we established a DEN + CCl$_4$ induced mice model of hepatic injury leading to the development of HCC. The reduced survival rate, poor health conditions and elevation of serum ALT/AST confirmed the successful hepatocellular tumour development (Nevzorova et al., 2020). Results also suggest the involvement of inflammation in the initiation and progression of hepatic damage leading to HCC as evident by stage specific regulation of suppressors of cytokine signalling and pro/anti-inflammatory mediators.

Di-ethyl-nitrosamine (DEN) is a carcinogenic chemical that can initiate liver damage whereas, CCl$_4$ is categorized as tumour promoting agent. Our results have shown that a combination of DEN + CCl$_4$ has successfully established hepatic injury to HCC mice model. High levels of serum ALT/AST were observed at different stages of HCC mice model. These results reflected the injury as comparable to the human HCC patients, where an increase of these enzymes is associated with augmented risk of HCC (Sarkar et al., 2020; Zhang et al., 2019b). Histopathological changes were significantly altered throughout the course of disease along with regulation of liver injury markers. The present results are comparable to previously reported combination of chemicals and chemically induced HCC rodent models (Wu et al., 2018, Zayed et al., 2019).

Cytochrome P450 pathway with heme containing proteins is mainly involved in the metabolism of drugs and toxicants (Esteves et al., 2021). Both DEN and CCl$_4$ are known to exacerbate liver functioning through regulation of cytochrome P450 and inflammatory signalling (Kovalszky et al., 1992, Ye et al., 2012, Li et al., 2014). Mice administered DEN + CCl$_4$ showed differential regulation of these hepatic cytochrome P450 genes (Cyp2e1, Cyp1a1 and Cyp1a2). These results are in accordance with previous

mice models and human HCC liver samples (Ho et al., 2004, Sun et al., 2019, Tripathy et al., 2020). Cyp2e1 and Cyp1a2 showed significantly reduced expression throughout the course of disease (Leung et al., 2013, García-Suástegui et al., 2017). Reduced expression of these enzymes has been suggested to induce oxidative radicals accelerating hepatic damage (Zhao et al., 2008, Lee et al., 2011). In contrast, the overexpression of Cyp1a1 has been documented which is known to stimulates endogenous lipid peroxidation resulting in accumulation of lipids (Boll et al., 2001, Shirakami et al., 2012, Huang et al., 2018). Continued generation of lipid metabolites lead to cellular damage, production of inflammatory cytokines and inflammatory responses (Ramos-Tovar and Muriel 2020).

Inflammatory signalling characterized by regulation of mediators and modulators play crucial role in hepatic microenvironment and injury (Abdulkhaleq et al., 2018, Huang et al., 2020). The balance between pro-inflammatory and anti-inflammatory responses can determine the development and progression of HCC (Dai et al., 2021). Here, especially the regulation of SOCS molecules as modulators of inflammatory responses have drawn attention in the pathogenesis of HCC (Fujimoto and Naka 2010, Rossa et al., 2012). In current results, the downregulation of Socs2/Socs3 along with upregulation of cytokines at early stages of hepatic injury highlights the role of inflammatory response modulation in hepatic damage. It has been reported that inhibition of SOCS could activate different oncogenic signalling pathways (Cui et al., 2016, Khan et al., 2020, Liu et al., 2021). Regulation of inflammatory cytokines have shown to promote HCC in animal models (Yu et al., 2010, Zhang et al., 2012). These result are also consistent with clinical investigation of human HCC (Kim et al., 2013).

TLRs signalling is a critical mechanism in immune responses and is activated by ligands such as lipopolysaccharides, free fatty acid, denatured DNA, endogenous proteins and oligonucleotides. TLRs activation is accompanied by damage associated molecular receptors (Zhang et al., 2010). The members of SOCSs family are also known to regulate TLRs signalling and participate in progression of HCC (Yu et al., 2010, Lopes et al., 2016). Enhanced expression was observed in advance stages of our hepatic injury mice. Previous studies also highlight the role of Tlrs regulation as chronically associated with DEN + CCl$_4$ induced HCC mice model (Dapito et al., 2012). It has been established that during HCC development, hepatocytes continuously undergo necrosis/apoptotic events and release fragmented DNA. This apoptotic DNA works as a ligand for TLR9 activation and contributes in the HCC progression (Watanabe et al., 2007). MYD88 is an adaptor protein of TLRs is required to stimulate TLRs signalling mediated inflammatory responses (Yuan et al., 2021). Specifically, TLRs signalling is involved in the regulation of pro-inflammatory cytokines (IL1-β, IL6 and/or TNF-α) and anti-inflammatory cytokines (IL-10, IL-12 and/or TGF-β) facilitated inflammation. Similarly like Tlrs, the expression of Myd88 is also augmented at advanced stages of hepatic injury along with enhanced inflammation. Previous studies also highlight the upregulaion of MYD88 in HCC (AbdAllah et al., 2021). It has also been reported that MYD88 mutant mice are protected from developing metabolic disruptions, atherosclerosis and liver fibrosis induced by DEN and CCl$_4$ (Naugler et al., 2007, Mohs et al., 2020).

Findings of current study designate the successful development of HCC as indicated by significant impairment of liver architecture and function. Results also highlight stage specific regulation of cellular and molecular events in the pathogenesis of HCC. Specifically, it is revealed that differential expression of Socs is associated with regulation of anti-inflammatory cytokines at each stage of hepatic injury. Therefore, it is concluded that Socs mediated inhibition of anti-inflammatory signalling plays a role in the initiation and progression of hepatic damage leading to HCC.

Declaration of Competing Interest

The authors declare that they have no known competing financial interests or personal relationships that could have appeared to influence the work reported in this paper.

Appendix A. Supplementary data

Supplementary data to this article can be found online at https://doi.org/10.1016/j.sjbs.2022.103348.

References

AbdAllah, N.B., Toraih, E.A., Al Ageeli, E., Elhagrasy, H., Gouda, N.S., Fawzy, M.S., Helal, G.M., 2021. Myd88, nfkb1, and il6 transcripts overexpression are associated with poor outcomes and short survival in neonatal sepsis. Sci. Rep. 11 (1). https://doi.org/10.1038/s41598-021-92912-7.

Abdulkhaleq, L.A., Assi, M.A., Abdullah, R., Zamri-Saad, M., Taufiq-Yap, Y.H., Hezmee, M.N.M., 2018. The crucial roles of inflammatory mediators in inflammation: A review. Vet. World 11 (5), 627–635.

Azam, F., Sheikh, N., Ali, G., Tayyeb, A., 2018. Fagonia indica repairs hepatic damage through expression regulation of toll-like receptors in a liver injury model. J. Immunol. Res. 2018, 1–12.

Bligh, E.G., Dyer, W.J., 1959. A RAPID METHOD OF TOTAL LIPID EXTRACTION AND PURIFICATION. Can. J. Biochem. Physiol. 37 (8), 911–917.

Boll, M., Weber, L.W., Becker, E., Stampfl, A., 2001. Mechanism of carbon tetrachloride-induced hepatotoxicity. Hepatocellular damage by reactive carbon tetrachloride metabolites. Z. Naturforsch. C. J. Biosci. https://doi.org/10.1515/znc-2001-7-826.

Chen, L., Deng, H., Cui, H., Fang, J., Zuo, Z., Deng, J., Li, Y., Wang, X., Zhao, L., 2018. Inflammatory responses and inflammation-associated diseases in organs. Oncotarget. 9 (6), 7204–7218.

Cui, M., Sun, J.i., Hou, J., Fang, T., Wang, X., Ge, C., Zhao, F., Chen, T., Xie, H., Cui, Y., Yao, M., Li, J., Li, H., 2016. The suppressor of cytokine signaling 2 (socs2) inhibits tumor metastasis in hepatocellular carcinoma. Tumor Biol. 37 (10), 13521–13531.

Dai, L., Li, Z., Tao, Y., Liang, W., Hu, W., Zhou, S., Fu, X., Wang, X., 2021. Emerging roles of suppressor of cytokine signaling 3 in human cancers. Biomed. 144, 112262. https://doi.org/10.1016/j.biopha.2021.112262.

Dapito, D., Mencin, A., Gwak, G.-Y., Pradere, J.-P., Jang, M.-K., Mederacke, I., Caviglia, J., Khiabanian, H., Adeyemi, A., Bataller, R., Lefkowitch, J., Bower, M., Friedman, R., Sartor, R.B., Rabadan, R., Schwabe, R., 2012. Promotion of hepatocellular carcinoma by the intestinal microbiota and tlr4. Cancer Cell. 21 (4), 504–516.

Esteves, F., Rueff, J., Kranendonk, M., 2021. The central role of cytochrome p450 in xenobiotic metabolism—a brief review on a fascinating enzyme family. J. Xenobiot. 11 (1), 94–114.

Fujimoto, M., Naka, T., 2010. Socs1, a negative regulator of cytokine signals and tlr responses, in human liver diseases. Gastroenterol. Res. Pract. 2010, 1–7.

García-Suástegui, W.A., Ramos-Chávez, L.A., Rubio-Osornio, M., Calvillo-Velasco, M., Atzin-Méndez, J.A., Guevara, J., Silva-Adaya, D., 2017. The role of cyp2e1 in the drug metabolism or bioactivation in the brain. Oxid. Med. Cell. Longevity 2017, 1–14.

Ghemrawi, R., Battaglia-Hsu, S.F., Arnold, C., 2018. Endoplasmic reticulum stress in metabolic disorders. Cells. https://doi.org/10.3390/cells7060063.

Ho, J.C., Cheung, S.T., Leung, K.L., Ng, I.O., Fan, S.T., 2004. Decreased expression of cytochrome p450 2e1 is associated with poor prognosis of hepatocellular carcinoma. Int. J. Cancer. 111 (4), 494–500.

Huang, B., Bao, J., Cao, Y.-R., Gao, H.-F., Jin, Y., 2018. Cytochrome p450 1a1 (cyp1a1) catalyzes lipid peroxidation of oleic acid-induced hepg2 cells. Biochemistry (Mosc.) 83 (5), 595–602.

Huang, S., Liu, K.e., Cheng, A., Wang, M., Cui, M., Huang, J., Zhu, D., Chen, S., Liu, M., Zhao, X., Wu, Y., Yang, Q., Zhang, S., Ou, X., Mao, S., Gao, Q., Yu, Y., Tian, B., Liu, Y., Zhang, L., Yin, Z., Jing, B.o., Chen, X., Jia, R., 2020. Socs proteins participate in the regulation of innate immune response caused by viruses. Frontiers 11. https://doi.org/10.3389/fimmu.2020.558341.

Irshad, M., Gupta, P., Irshad, K., 2017. Molecular basis of hepatocellular carcinoma induced by hepatitis c virus infection. WJH 9 (36), 1305–1314.

Jafri, W., Kamran, M., 2019. Hepatocellular carcinoma in Asia: A challenging situation. Euroasian J. Hepatogastroenterol. https://doi.org/10.5005/jp-journals-10018-1292.

Jiang, M., Zhang, W.-W., Liu, P., Yu, W., Liu, T., Yu, J., 2017. Dysregulation of socs-mediated negative feedback of cytokine signaling in carcinogenesis and its significance in cancer treatment. Frontiers. in immunology.

Khan, M.G.M., Ghosh, A., Variya, B., Santharam, M.A., Ihsan, A.U., Ramanathan, S., Ilangumaran, S., 2020. Prognostic significance of SOCS1 and SOCS3 tumor suppressors and oncogenic signaling pathway genes in hepatocellular carcinoma. BMC Cancer 20 (1). https://doi.org/10.1186/s12885-020-07285-3.

Kim, E., Viatour, P., 2020. Hepatocellular carcinoma: Old friends and new tricks. Exp. Mol. Med. 52 (12), 1898–1907.

Kim, M.J., Jang, J.W., Oh, B.S., Kwon, J.H., Chung, K.W., Jung, H.S., Jekarl, D.W., Lee, S., 2013. Change in inflammatory cytokine profiles after transarterial chemotherapy in patients with hepatocellular carcinoma. Cytokine. https://doi.org/10.1016/j.cyto.2013.07.021.

Kovalszky, I., Szeberenyi, S., Zalatnai, A., Vincze, I., Lapis, K., Jeney, A., 1992. Modification of dena-induced hepatocarcinogenesis by ccl4 cirrhosis. Comparison of the marker enzyme patterns. Carcinogenesis. https://doi.org/10.1093/carcin/13.5.773.

Lee, G.-H., Bhandary, B., Lee, E.-M., Park, J.-K., Jeong, K.-S., Kim, I.-K., Kim, H.-R., Chae, H.-J., 2011. The roles of er stress and p450 2e1 in ccl(4)-induced steatosis. Int. J. Biochem. Cell Biol. 43 (10), 1469–1482.

Leung, T., Rajendran, R., Singh, S., Garva, R., Krstic-Demonacos, M., Demonacos, C., 2013. Cytochrome p450 2e1 (cyp2e1) regulates the response to oxidative stress and migration of breast cancer cells. Breast Cancer Res. 15 (6). https://doi.org/10.1186/bcr3574.

Li, X.-X., Zheng, Q.-C., Wang, Y., Zhang, H.-X., 2014. Theoretical insights into the reductive metabolism of ccl4 by cytochrome p450 enzymes and the ccl4-dependent suicidal inactivation of p450. Dalton Trans. 43 (39), 14833–14840.

Liu, J., Liu, Z., Li, W., Zhang, S., 2021. Socs2 is a potential prognostic marker that suppresses the viability of hepatocellular carcinoma cells. Oncol. Lett. 21 (5). https://doi.org/10.3892/ol.2021.12660.

Lokau, J., Schoeder, V., Haybaeck, J., Garbers, C., 2019. Jak-stat signaling induced by interleukin-6 family cytokines in hepatocellular carcinoma. Cancers.

Lopes, J.A., Borges-Canha, M., Pimentel-Nunes, P., 2016. Innate immunity and hepatocarcinoma: Can toll-like receptors open the door to oncogenesis? Hepatol. World J. https://doi.org/10.4254/wjh.v8.i3.162.

Mohs, A., Kuttkat, N., Otto, T., Youssef, S.A., De, B.A., Trautwein, C., 2020. Myd88-dependent signaling in non-parenchymal cells promotes liver carcinogenesis. Carcinogenesis. https://doi.org/10.1093/carcin/bgy173.

Naugler, W.E., Sakurai, T., Kim, S., Maeda, S., Kim, KyoungHyun, Elsharkawy, A.M., Karin, M., 2007. Gender disparity in liver cancer due to sex differences in myd88-dependent il-6 production. Science. https:// 317 (5834), 121–124.

Nevzorova, Y.A., Boyer-Diaz, Z., Cubero, F.J., Gracia-Sancho, J., 2020. Animal models for liver disease - a practical approach for translational research. J. Hepatol. https://doi.org/10.1016/j.jhep.2020.04.011.

Omura, K.o., Uehara, T., Morikawa, Y., Hayashi, H., Mitsumori, K., Minami, K., Kanki, M., Yamada, H., Ono, A., Urushidani, T., 2014. Detection of initiating potential of non-genotoxic carcinogens in a two-stage hepatocarcinogenesis study in rats. J. Toxicol. Sci. 39 (5), 785–794.

Perveen, S., Ashfaq, H., Shahjahan, M., Manzoor, A., Tayyeb, A., 2020. Citrullus colocynthis regulates de novo lipid biosynthesis in human breast cancer cells. J. Cancer Res. Therap.

Ramos-Tovar, E., Muriel, P., 2020. Molecular mechanisms that link oxidative stress, inflammation, and fibrosis in the liver. Antioxidants 9 (12), 1279. https://doi.org/10.3390/antiox9121279.

Refolo, M.G., Messa, C., Guerra, V., Carr, B.I., D'Alessandro, R., 2020. Inflammatory mechanisms of hcc development. Cancers 12 (3), 641. https://doi.org/10.3390/cancers12030641.

Rossa, C., Sommer, G., Spolidorio, L.C., Rosenzweig, S.A., Watson, D.K., Kirkwood, K. L., Li, J., 2012. Loss of expression and function of socs3 is an early event in hnscc: Altered subcellular localization as a possible mechanism involved in proliferation, migration and invasion. PLoS ONE 7 (9), e45197. https://doi.org/10.1371/journal.pone.004519710.1371/journal.pone.0045197.g00110.1371/journal.pone.0045197.g00210.1371/journal.pone.0045197.g00310.1371/journal.pone.0045197.g00410.1371/journal.pone.0045197.g00510.1371/journal.pone.0045197.g006.

Sarkar, S., Bhattacharjee, P., Ghosh, T., Bhadra, K., 2020. Pharmaceutical efficacy of harmalol in inhibiting hepatocellular carcinoma. Future. J. Pharm. Sci. 6 (1). https://doi.org/10.1186/s43094-020-00045-x.

Shirakami, Y., Gottesman, M.E., Blaner, W.S., 2012. Diethylnitrosamine-induced hepatocarcinogenesis is suppressed in lecithin: Retinol acyltransferase-deficient mice primarily through retinoid actions immediately after carcinogen administration. Carcinogenesis 33 (2), 268–274.

Sobah, M.L., Liongue, C., Ward, A.C., 2021. Socs proteins in immunity, inflammatory diseases, and immune-related cancer. Front. Med.

Stanke-Labesque, F., Gautier-Veyret, E., Chhun, S., Guilhaumou, R., Pharmacology, F. S.o., Therapeutics,, 2020. Inflammation is a major regulator of drug metabolizing enzymes and transporters: Consequences for the personalization of drug treatment. Pharmacol. Ther.

Sun, J., Wang, J., Zhang, N., Yang, R., Chen, K., Kong, D., 2019. Whole transcriptome analysis of chemically induced hepatocellular carcinoma using rna-sequencing analysis. FEBS Open Bio. https://doi.org/10.1002/2211-5463.12724.

Sung, H., Ferlay, J., Siegel, R.L., Laversanne, M., Soerjomataram, I., Jemal, A., Bray, F., 2021. Global cancer statistics 2020: Globocan estimates of incidence and mortality worldwide for 36 cancers in 185 countries. CA A Cancer J. Clin. 71 (3), 209–249.

Suresh, D., Srinivas, A.N., Kumar, D.P., 2020. Etiology of hepatocellular carcinoma: Special focus on fatty liver disease. Oncol. Front. https://doi.org/10.3389/fonc.2020.601710.

Tripathy, A., Thakurela, S., Sahu, M.K., Uthansingh, K., Singh, A., Narayan, J., Ajay, A. K., Singh, V., Kumari, R., 2020. Fatty changes associated with n-nitrosodiethylamine (den) induced hepatocellular carcinoma: A role of sonic hedgehog signaling pathway. Genes Cancer. 11 (1-2), 66–82.

Watanabe, A., Hashmi, A., Gomes, D.A., Town, T., Badou, A., Flavell, R.A., Mehal, W.Z., 2007. Apoptotic hepatocyte DNA inhibits hepatic stellate cell chemotaxis via toll-like receptor 9. Hepatology 46 (5), 1509–1518.

Wu, Q., Chen, J.-X., Chen, Y.u., Cai, L.-l., Wang, X.-Z., Guo, W.-H., Zheng, J.-F., 2018. The chemokine receptor ccr10 promotes inflammation-driven hepatocarcinogenesis via pi3k/akt pathway activation. Cell Death Dis 9 (2). https://doi.org/10.1038/s41419-018-0267-9.

Yang, Y., Kim, S.o., Seki, E., 2019. Inflammation and liver cancer: Molecular mechanisms and therapeutic targets. Semin. Liver Dis. 39 (01), 026–042.

Ye, C., Driver, J.P., 2016. Suppressors of cytokine signaling in sickness and in health of pancreatic β-cells. Front. Immunol.

Ye, Q., Lian, F., Chavez, P.R., Chung, J., Ling, W., Qin, H., Seitz, H.K., Wang, X.D., 2012. Cytochrome p450 2e1 inhibition prevents hepatic carcinogenesis induced by diethylnitrosamine in alcohol-fed rats. Hepatobiliary Surg. Nutr. https://doi.org/10.3978/j.issn.2304-3881.2012.11.05.

Yu, L.-X., Ling, Y., Wang, H.-Y., 2018. Role of nonresolving inflammation in hepatocellular carcinoma development and progression. npj Precision Onc 2 (1). https://doi.org/10.1038/s41698-018-0048-z.

Yu, L.-X., Yan, H.-X., Liu, Q., Yang, W., Wu, H.-P., Dong, W., Tang, L., Lin, Y., He, Y.-Q., Zou, S.-S., Wang, C., Zhang, H.-L., Cao, G.-W., Wu, M.-C., Wang, H.-Y., 2010. Endotoxin accumulation prevents carcinogen-induced apoptosis and promotes liver tumorigenesis in rodents. Hepatology 52 (4), 1322–1333.

Yuan, G., Chen, B., Meng, Y., Lu, J., Shi, X., Hu, A., Hu, Y., Wang, D., 2021. Role of the cxcr3-mediated tlrs/myd88 signaling pathway in promoting the development of hepatitis b into cirrhosis and liver cancer. Mol. Med. Rep.

Zayed, M.N., Aly, H.F., Moneim El-Mezayen, H.A., El-Salamony, H.E., 2019. Effect of co-administration of bee honey and some chemotherapeutic drugs on dissemination of hepatocellular carcinoma in rats. Toxicol. Rep. https://doi.org/10.1016/j.toxrep.2019.08.007.

Zhang, H.E., Henderson, J.M., Gorrell, M.D., 2019a. Animal models for hepatocellular carcinoma. Biochim. Biophys. Acta (BBA) – Mol. Basis Disease 1865 (5), 993–1002.

Zhang, H.L., Yu, L.X., Yang, W., Tang, L., Lin, Y., Wu, H., Zhai, B., Tan, Y.X., Shan, L., Liu, Q., Chen, H.Y., Dai, R.Y., Qiu, B.J., He, Y.Q., Wang, C., Zheng, L.Y., Li, Y.Q., Wu, F.Q., Li, Z., Yan, H.X., Wang, H.Y., 2012. Profound impact of gut homeostasis on chemically-induced pro-tumorigenic inflammation and hepatocarcinogenesis in rats. J. Hepatol. https://doi.org/10.1016/j.jhep.2012.06.011.

Zhang, L.-X., Lv, Y., Xu, A.-M., Wang, H.-Z., 2019b. The prognostic significance of serum gamma-glutamyltransferase levels and ast/alt in primary hepatic carcinoma. BMC Cancer 19 (1). https://doi.org/10.1186/s12885-019-6011-8.

Zhang, Q., Raoof, M., Chen, Y.u., Sumi, Y., Sursal, T., Junger, W., Brohi, K., Itagaki, K., Hauser, C.J., 2010. Circulating mitochondrial damps cause inflammatory responses to injury. Nature 464 (7285), 104–107.

Zhao, X., Zhang, J.-J., Wang, X., Bu, X.-Y., Lou, Y.-Q., Zhang, G.-L., 2008. Effect of berberine on hepatocyte proliferation, inducible nitric oxide synthase expression, cytochrome p450 2e1 and 1a2 activities in diethylnitrosamine- and phenobarbital-treated rats. Biomed. Pharmacother. 62 (9), 567–572.